Satellite-observed cloud and precipitation patterns in Southeast Asia during the monsoon onset period and their interannual variations

Po-Chia Chen, Wen-Hai Ling
Department of Atmospheric Sciences,
National Taiwan University

Abstract

In this study, we use the TRMM precipitation data, the ISCCP cloud amounts (CA) and weather state (WS) to illustrate the change in clouds and precipitation in the Southeast Asian region during summer monsoon onset period. The South China Sea summer monsoon (SCSSM) index is used as an indicator of the transition of the summer monsoon, and the Real-Time Multivariate MJO (RMM) index provided by Bureau of Meteorology in Australian is used to define the Madden–Julian oscillation (MJO) phase and analyze the MJO influence on the changes of cloud, precipitation and wind circulation during the summer monsoon onset period and the development of MJO.

Key word: South China sea Summer monsoon, ISCCP, satellite-observed cloud amount, intraseasonal oscillation

1. Introduction

The East Asian summer monsoon and related seasonal rain belts assumes significant variability at intraseasonal, interannual and interdecadal time scales[1]. After the onset of the Asian summer monsoon, the moisture transport coming from the Indochina Peninsula and the South China Sea plays a crucial ”switch” role in moisture supply for precipitation in East Asia[1]. In addition, the onset of South China Sea monsoon (SCSM) could be viewed as the first transition of Asian summer monsoon (ASM) causing major changes in both convection and winds[2].

Besides winds and precipitation, the radiation is another index often used to diagnose the monsoon onset. Joseph et al, 2006[3] showed a decrease in OLR which is 10 days prior to the MOK in India region. While previous studies showing robust relation between monsoon onsets between winds, precipitation or radiation, seldom of them used the cloud types or cloud amount to illustrate the monsoon onset.

The tropical intraseasonal oscillation also plays an important role in the monsoon onset. In Hung and Hsu (2008)[4], it shows the sharp onset of the ASM tends to occur concurrently with the strong TISO signal in most of the years, and indicates intraseasonal oscillation might be associated with the monsoon onset. In Benedict and Randall (2007)[5], the MJO schematics diagram of clouds shows the evolution of cloud types through MJO phases. The evolution clouds through MJO phases starts from shallow clouds to deep convection and thick clouds, and then returns to shallow clouds. Therefore, we try to find if the cloud evolution during the monsoon onset is consistent with the MJO schematics diagram.

As a consequence, we try to discover the relation between the winds, clouds and precipitation in Southeast Asia during the monsoon-onset period via the satellite-observed datasets, and try to understand their intraseasonal variations.

In this study, we use the TRMM precipitation data, the ISCCP cloud amounts (CA) and weather state (WS) to illustrate the change in clouds and precipitation in the Southeast Asian region, as well as the interactions with the Madden–Julian oscillation (MJO) phase changes and development during the summer monsoon onset period.

2. Data and Resources

The International Satellite Cloud Climatology Project (ISCCP) provides various datasets of satellite observation. In our study, we use the ISCCP HGG-Cloud Amount (CA) to analyze the change of different kinds of clouds over the domain, with the temporal coverage from 1984 to 2016. Due to the observation limitation, only the daily UTC 0300 data is used albeit the interval of the original data is every three hours. The original HGG-CA data is a Pc -Tau (Cloud top pressure-optical depth) histogram for each 1-degree grid box, with the dimension of 7x6. It contains the distribution of cloud fraction among the 7x6 intervals of cloud properties. By adding the distribution respectively, the cloud amount of each 9 types of ICCP clouds could be obtained.

In addition, the ISCCP Cloud Regime/Weather State (WS) data is used to illustrate the evolution of different cloud components combinations, with the interval of every three hours and temporal coverage from 1984 to 2015. The spatial resolution of the WS data is

1-degree, with 1 of 10 possible Cloud Regime/Weather State on each grid. It is worth noting that the listing order of the WS is quite different from the aforementioned 9 types of ISCCP clouds.

The TRMM daily precipitation rate is in use, with the temporal coverage from 1998 to 2017 and spatial resolution of 0.25-degree. The daily outgoing longwave radiation dataset (OLR) from NOAA is used as well.

The ERA5 reanalysis dataset of zonal wind component at 850 hPa level (U850) with the interval of every 12 hours is used in order to define the SCSSM index afterwards. Plus, the daily Real-Time Multivariate MJO (RMM) index, provided by the Bureau of Meteorology in Australia, is used to define the Madden–Julian oscillation (MJO) phase.

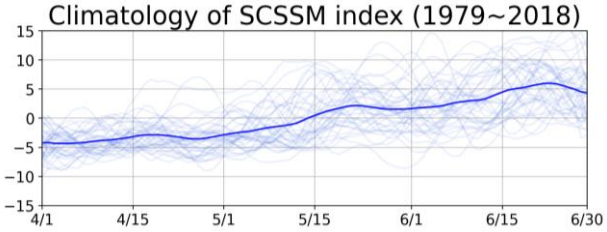

Fig. 1. The climatology of SCSSM index from 1979 to 2018. Thin lines show the evolution for each year, while the thick line represents the mean evolution.

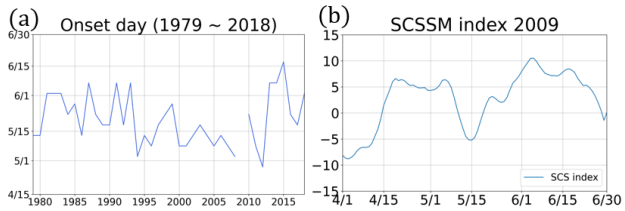

Fig. 2. (a) The onset day which is defined by Wang et al (2004) from 1979 to 2018. (b) The SCSSM index in 2009, which changes sign in the mid-April, is unsuitable to define the onset day.

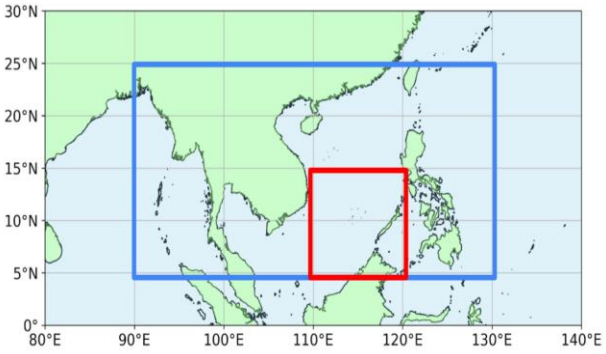

Fig. 3. The region of Southeast-Asia (5°N–25°N, 90°E–130°E) in blue box and South China Sea region (5°N–15°N, 110°E–120°E) in red box.

3. Methodology

A. Defining monsoon onset

The SCS summer monsoon (SCSSM) onset indeed signifies the beginning of the summer monsoon over East Asia and the adjacent western Pacific Ocean[6]. We follow the definition in Wang et al, 2004[6], defining the SCSSM Index (USCS) as the 850-hPa zonal winds averaged over the region of South China Sea (5°N–15°N, 110°E–120°E).

The onset date for each year is defined by the first pentad after 25 April that satisfies the following two criteria:

a. the onset pentad USCS > 0 m/s.

b. in the subsequent four pentads (including the onset pentad) USCS must be positive in at least three pentads and the accumulative four pentad mean USCS > 1 m/s.

The climatology of SCSSM index changes to positive during mid-May as shown in Fig. 1., and the exact onset day for each year is presented in Fig. 2a as well.

The index in 2009 (Fig. 2b) is unsuitable to define the onset day by the definition, since the positive index started from April 15. The phenomenon might be a result from the La Niña event in the previous year, so we ignore it when we do the composite analysis.

B. Southeast Asia and China Sea Region

We select two regions in this research, one is Southeast Asia (5°N–25°N, 90°E–130°E), which is represented as the blue box in Fig. 3, the other is the South China Sea region (5°N–15°N, 110°E–120°E), which is represented as the red box in Fig. 3. The red box is focued on South China Sea by following the region selected in the Wang et al, 2004[6]. The blue box is selected in order to cover the entire South China Sea and extends to the Indochina Peninsula and adjacent waters.

C. The Composite Analysis

The aforementioned onset date for each year is used as the standard to adjust the time to the same in order to obtain the composite analysis for each variable. For example, for the year of onset date which is 10 days later than the mean onset date, the variable data in that year would be rolled 10 days forward in order to align the onset day. By this method, the time difference of the annual transition can be eliminated, so we can focus more on the changes in the monsoon onset.

4. Results

A. Precipitation

The zonal mean of climatology precipitation in 90°E-130°E and 110°E-120°E are presented as Fig. 4a and Fig. 4b, and the composite precipitation in 90°E-130°E and 110°E-120°E are presented as Fig. 4c and Fig. 4d. The climatology precipitation has an increase between 5-20°N after mid-May due to the monsoon onset in Fig. 4a, 4b, 4c and 4d. The phenomenon is clearer in composite analysis. Compared to the climatology precipitation, the composite precipitation has a more obvious northward jump from -5°S-5°N to 5°N-15°N in mid-May.

B. ISCCP Cloud Amount (CA)

The time-series for 9 kinds of clouds are shown in Fig. 5. The left panels show the CA evolutions over the Southeast-Asia region (5°N–25°N, 90°E–130°E), while the right panels show the average over the South China Sea region (5°N–15°N, 110°E–120°E). The upper panels are the climatology, and the lower panels are the composite results. It's obvious that the evolutions for the high-clouds (Ci, Cs, DC) are more related to the change in precipitation during the monsoon-onset. For instance, the Cs and DC increase drastically around the onset day compared to other types of clouds in the composite results. In addition, the significant increase in the Ci is about 20 days earlier than the monsoon-onset, which implies there is a lead-lag relationship exists.

The zonal mean (90°E-130°E) composite results of the CA for Ci, Cs and DC are presented in Fig. 6 (a), (b) and (c), respectively. It could be observed that an increase in Ci among 5°N-20°N is about 20 days earlier than the onset day. On the other hand, the DC shows a clearer northward jump taking place just on the onset day. In contrast, the Cs shows a continuous northward movement. The results in Fig.6 indicate the onset day could not only be used as an indicator for the change of CA in the 5°N-20°N region, but also be viewed as the indicator for the sudden drop of CA in the 10°S-0° region.

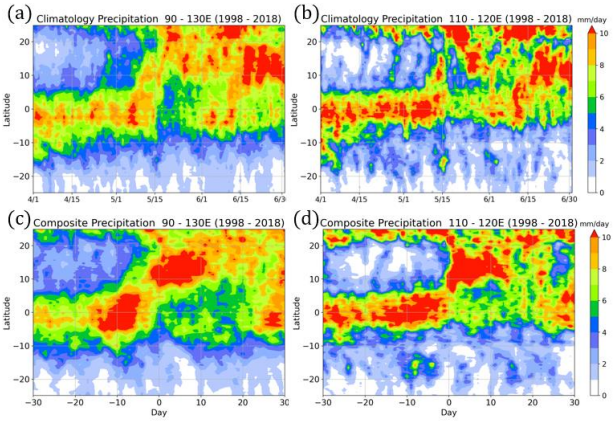

Fig. 4. The zonal mean of climatology precipitation 1998 - 2017 in 90°E-130°E (a) and 110°E-120°E (b). The zonal mean of composite precipitation 1998 - 2017 in 90°E-130°E (c) and 110°E-120°E (d).

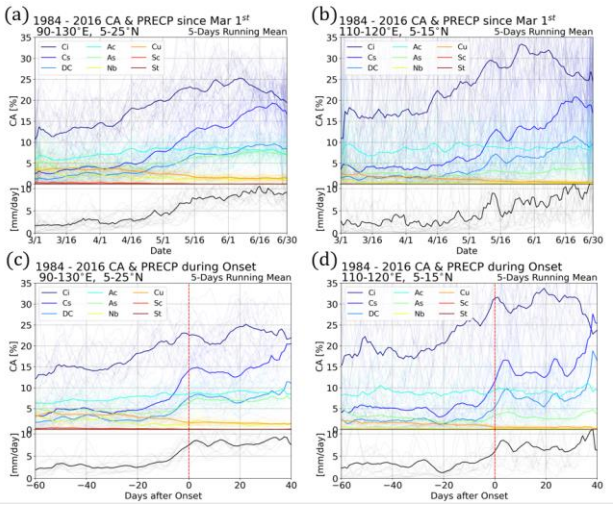

Fig. 5. The 5- day running mean of ISCCP Cloud Amount (1984 - 2016) and precipitation (1998 - 2017) in Southeast-Asia [90°E-130°E, 5°N-25°N] (a) and South China Sea [110°E-120°E, 5°N-15°N] (b). The composite ISCCP Cloud Amount (1984 - 2016) and precipitation (1998 - 2017) in Southeast-Asia [90°E-130°E, 5°N-25°N] (c) and South China Sea [110°E-120°E, 5°N-15°N] (d). The solid lines show the evolution of nine clouds. The light solid color lines show the evolution for each year of nine clouds.

C. ISCCP Weather State (WS)

The time-series of the ISCCP Weather State during the monsoon onset is presented as Fig. 7. The left panels show the average over the Southeast-Asia region (5°N–25°N, 90°E–130°E), while the right panels show the average over the South China Sea region (5°N–15°N, 110°E–120°E). The upper panels are the climatology, and the lower panels are the composite results. It shows that the WS7 decreases with time while the WS1 increases gradually. The other WSs have no significant trends. It seems that WS1 and WS7 are the two types of main weather patterns in Southeast-Asia.

The cloud top pressure-τ distributions for the WS1 and WS7 are presented in Fig. 8(a) and (b). The clouds with higher tops in the WS1 represent that the clouds is more related to the convective system and severe precipitation, while the lower clouds in WS7 indicate a more convective-suppressed atmosphere condition. The composite time-latitude diagrams of WS1 and WS7 are presented in Fig. 9(a) and (b). The phenomenon of increasing trend in WS1 in 5°N-15°N and decrease in WS7 in 10°N-20°N during monsoon onset period could be observed in Fig. 9. The latitude range of increase in WS1 and decrease in WS7 are slightly different. The growth in WS1 and decline in WS7 shows the convective process is more active during the monsoon onset period, which is consistent with the previous analysis.

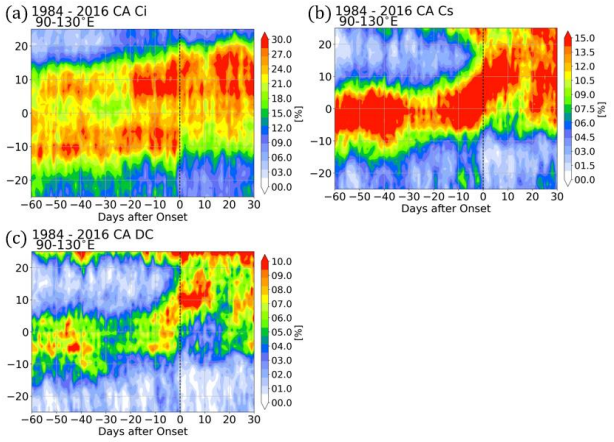

Fig. 6. The zonal mean of composite Cirrus (a), Cirrostratus (b) and Deep convective (c) in 90°E-130°E during 1984-2016.

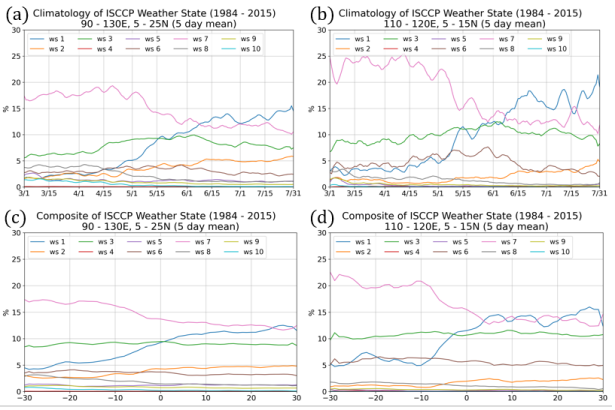

Fig. 7. The 5- day running mean of ISCCP Weather State (1984 - 2015) in Southeast-Asia [90°E-130°E, 5°N-25°N] (a) and South China Sea [110°E-120°E, 5°N-15°N] (b). The composite ISCCP Cloud Amount (1984 - 2016) and precipitation (1998 - 2017) in Southeast-Asia [90°E-130°E, 5°N-25°N] (c) and South China Sea [110°E-120°E, 5°N-15°N] (d). The solid lines show the evolution of ten weather states.

D. Monsoon onset with intraseasonal oscillations

In this study, we choose the Madden–Julian oscillation as a representative intraseasonal oscillation, since it's the major fluctuation in tropical weather on weekly to monthly timescales. We use the Real-Time Multivariate MJO (RMM) index provided by the Bureau of Meteorology in Australia to define the Madden–Julian oscillation (MJO) phase. The MJO phase defined by RMM1 and RMM2 shows the evolution and location of the MJO along the equator. We analyze the MJO phase during the summer monsoon onset period from 1979 to 2018, and the result is presented in Fig. 10. There is a 50% chance that the MJO phase is located near the Indian Ocean (phase 2 and 3) ten days before onset, and 60% chance that MJO phase is located in the Maritime Continent (phase 4 and 5) near the monsoon onset day. It shows that the intraseasonal oscillations play an important role before the summer monsoon onset.

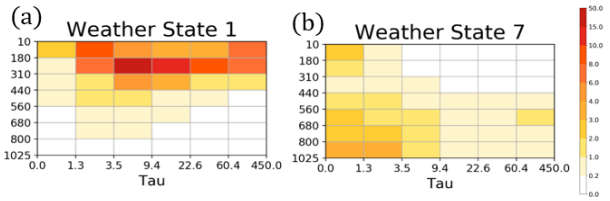

Fig. 8. The Pc -Tau histograms of Weather State 1 (a) and Weather State 7 (b).

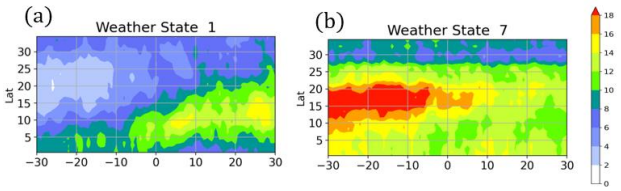

Fig. 9. The zonal mean of composite ISCCP Weather State 1 (a) and Weather State 7 (b) in 90°E-130°E during 1984-2015.

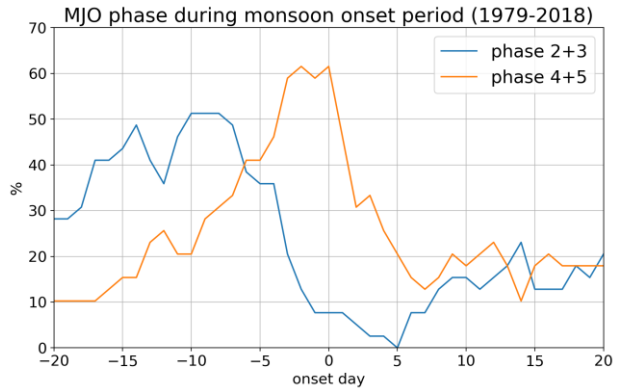

Fig. 10. MJO phase during the summer monsoon onset period from 1979 to 2018.

In order to find the influences of intraseasonal oscillations on summer monsoon onset, we choose years that the MJO is considered more active and strong by using the RMM index. We calculate the RMM mean amplitude from 15 days before onset date to the onset date, and the result is presented in Fig. 11. We choose the year that the RMM mean amplitude is greater than 1.5 as representative years. In these years, we remove 1998, since the year is mostly affected by the ENSO event, and some other years which have no ISCCP cloud data. Finally, the years we choose are 1987, 1990, 1991, 1993, 1995, 2002, 2003, 2004, 2005, 2011 and 2015, a total of eleven years. We analyze the outgoing longwave radiation (OLR) in the selected eleven years.

The average OLR anomaly of selected 11 years between 5°S and 5°N is presented in Fig. 12. The eastward propagation of negative OLR anomaly from the Indian Ocean to the Western Pacific can be seen clearly in the figure during the summer monsoon onset period, which indicates there is a convection signal of MJO. Besides, we analyze the cloud, precipitation patterns and wind circulation during the summer monsoon onset period in these years, trying to find the development and influence of MJO on Southeast Asia before summer monsoon onset.

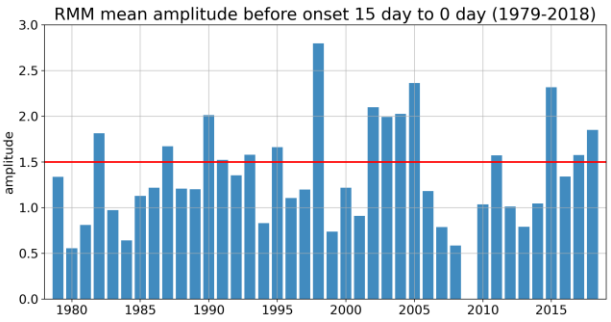

Fig. 11. RMM mean amplitude from 15 days before onset date to the onset date. The red line represents the threshold we choose.

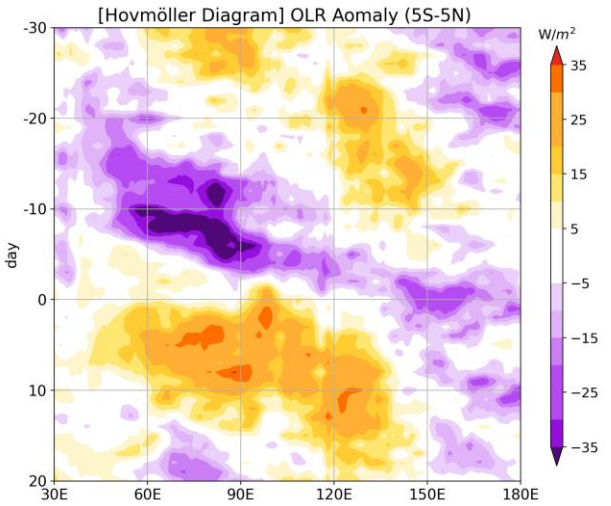

Fig. 12. The average OLR anomaly Hovmöller diagram of selected 11 years (1987, 1990, 1991, 1993, 1995, 2002, 2003, 2004, 2005, 2011 and 2015) between 5°S and 5°N.

In the following analysis, we choose four regions as representative. The four regions are East of Indian Ocean, Maritime Continent, Bay of Bengal and South China Sea, respectively, which are represented in Fig. 13. The composite results of the ISCCP cloud amount during the summer monsoon onset period are presented in Fig. 14 for only cirrus(Ci), cirrostratus (Cs) and deep convection (DC), since the change of the other cloud types are not significant. The precipitation is also presented in Fig. 14. The time-series of the results in East of Indian Ocean, Maritime Continent, Bay of Bengal and South China Sea are presented in Fig. 14 (a), (b), (c) and (d), respectively.

In East of Indian Ocean, cirrus, cirrostratus and deep convection begin to increase about 20 days earlier than the onset day. Cirrus reach their highest point in about day -10, and altostratus and deep convection reach their highest point in about day -5 days. In the Maritime Continent, the change of clouds lag behind in the East of the Indian Ocean by about 5-10 days. In Bay of Bengal, the change of clouds lag behind the Indian Ocean by about 10 days. In South China Sea, the change of clouds lagged behind Bay of Bengal by about 5 days. The development of clouds and convection in different regions lag between each other about 5-10 days. In the development of clouds and convection process, the beginning of the increase in cirrus is earlier than cirrostratus and deep convection for about 10 days.

From the OLR anomaly Hovmöller diagram and the lead-lag relationship of cloud development, it shows that a MJO convective phase passes through the Indian Ocean about 10 days earlier than the onset day, and gradually propagates eastward into Maritime Continent. The development of clouds and convection subsequently propagates northward into Bay of Bengal, and then moves eastward into South China Sea, causing the beginning of the SCS summer monsoon.

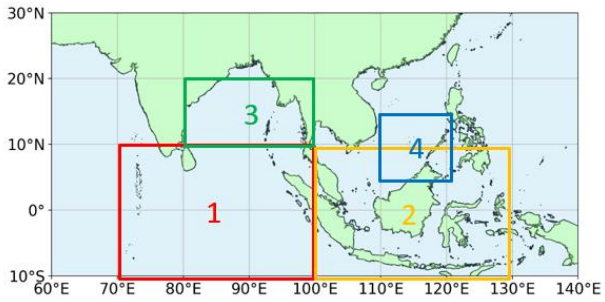

Fig. 13. The region of East of Indian Ocean (-10°N–10°N, 70°E–100°E) in red box, Maritime Continent (-10°N–10°N, 100°E–130°E) in yellow box, Bay of Bengal (10°N–20°N, 80°E–100°E) in green box and South China Sea region (5°N–15°N, 110°E–120°E) in blue box.

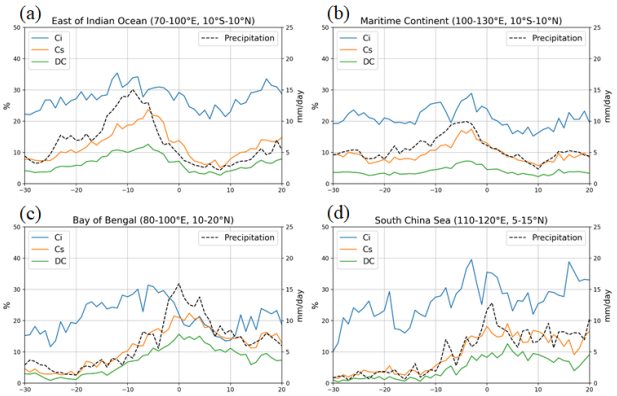

Fig. 14. The time series of ISCCP Cloud Amount (1987, 1990, 1991, 1993, 1995, 2002, 2003, 2004, 2005, 2011, 2015) for cirrus (Ci), cirrostratus (Cs) and deep convection (DC) and precipitation (2002, 2003, 2004, 2005, 2011, 2015) in East of Indian Ocean (a), Maritime Continent (b), Bay of Bengal (c) and South China Sea (d)

5. Summary and Discussion

In the analysis of ISCCP Cloud Amount during summer monsoon onset over the Southeast Asia, the increase in Ci is about twenty days earlier than the monsoon-onset, Cs shows a continuous northward movement, and the northward jump in DC is similar to the precipitation, while other cloud types have no significant change. In general, the evolutions for the high-clouds (Ci, Cs, DC) are more related to the change in precipitation. The earlier increase in Ci may be used as a prediction for the following monsoon onset in the South China Sea.

In ISCCP Weather State analysis, we find that during monsoon onset period, only WS 1 increases and

WS 7 decreases, while other WSs have no significant change. We think that it might be that the classification of weather states is based on global regions. We think that we could separate the weather states in Southeast-Asia into more detailed types and analyze their trends.

In the analysis of the intraseasonal oscillations during summer monsoon, we find the MJO is often observed before the summer monsoon onset. We choose eleven years which the MJO is observed before onset, trying to find the influences of intraseasonal oscillations on summer monsoon onset. In these years, an MJO convective phase passes through the Indian Ocean about 10 days earlier before the onset day, and then propagates eastward and northward. When the MJO convective phase passes through the Maritime Continent and South China Sea, the SCS monsoon onset process begins, accompanied with the change of wind from easterly to westerly, the increase in high clouds and precipitation.

The lead-lag relationship of clouds and precipitation indicates that an intraseasonal oscillation exists before SCS monsoon onset, and it plays an important role to the beginning of the SCS summer monsoon.

6. Reference

1. Yihui, D., & Chan, J. C., 2005:"The East Asian summer monsoon: an overview",Meteorology and Atmospheric Physics, 89(1),117-142
2. Hsu, H. H., Terng, C. T., & Chen, C. T., 1999:" Evolution of large-scale circulation and heating during the first transition of Asian summer monsoon",Journal of Climate,12(3),793-810
3. Joseph, P. V., Sooraj, K. P., & Rajan, C. K., 2006:" The summer monsoon onset process over South Asia and an objective method for the date of monsoon onset over Kerala",International Journal of Climatology: A Journal of the Royal Meteorological Society,26(13),1871-1893
4. Hung, C. W., & Hsu, H. H., 2008:"The first transition of the Asian summer monsoon, intraseasonal oscillation, and Taiwan mei-yu",Journal of climate,21(7),1552-1568
5. Benedict, J. J., & Randall, D. A. (2007). Observed characteristics of the MJO relative to maximum rainfall. Journal of Atmospheric Sciences, 64(7), 2332-2354.
6. Wang, B., Zhang, Y., & Lu, M. M., 2004:"Definition of South China Sea monsoon onset and commencement of the East Asia summer monsoon",Journal of Climate,17(4),699-710

7. Appendix

1. ISCCP Cloud type

The original HGG-CA data at each time step is a Pc -Tau (Cloud top pressure-optical depth) histogram (Fig. 15) for each 1-degree grid box, with the dimension of 7x6. It contains the distribution of cloud fraction among the 7x6 intervals of cloud properties. By adding the distribution respectively (Fig. 16), the cloud amount of each 9 types of ICCP clouds could be obtained.

2. ISCCP Cloud Regime/Weather State

Based on the aforementioned Pc -Tau histogram dataset, a series of categories of the histogram centroids (Fig. 17) could be obtained via the k-means cluster analysis. These 10 types of cloud regimes represent the common combinations of different types of clouds, which named as "weather state" as well. The 11th type of weather state is clear sky.

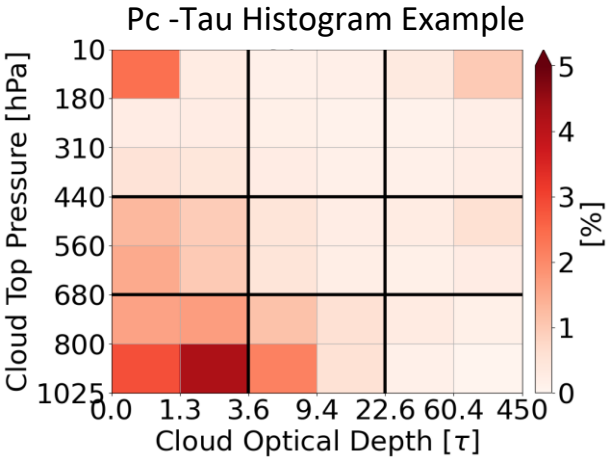

Fig. 15. Pc-Tau histogram example. The thick black lines indicate the dividing lines between different types of clouds.

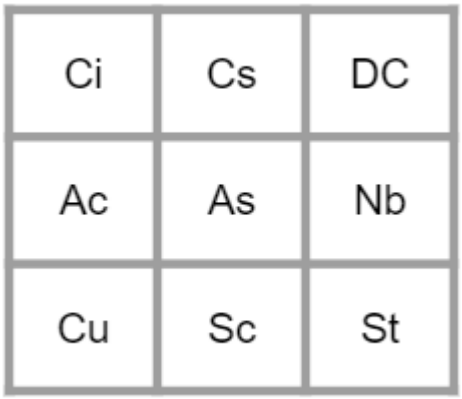

Fig. 16. ISCCP cloud types. The 9-square division corresponds to the black dividing lines in the Fig. 15.

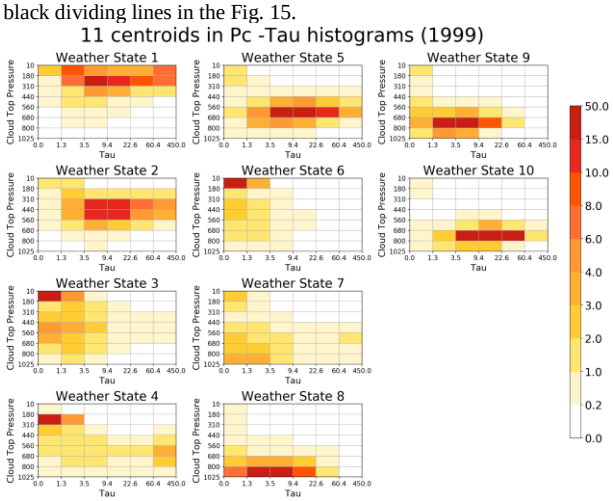

Fig. 17. ISCCP cloud regime/weather state histogram centroids.